

US EPA ARCHIVE DOCUMENT



**US Army Corps
of Engineers®**
Engineer Research and
Development Center

Modeling the Transport of Oil Particle Aggregates and Mixed Sediment in Surface Waters

February 2015

Earl Hayter, Richard McCulloch, Todd Redder, Michel Boufadel, Rex Johnson, and Faith Fitzpatrick

U.S. Army Corps of Engineers
Engineer Research and Development Center
Environmental Laboratory
3909 Halls Ferry Road
Vicksburg, MS 39180

Letter Report

The US Army Engineer Research and Development Center (ERDC) solves the nation's toughest engineering and environmental challenges. ERDC develops innovative solutions in civil and military engineering, geospatial sciences, water resources, and environmental sciences for the Army, the Department of Defense, civilian agencies, and our nation's public good. Find out more at www.erd.c.usace.army.mil.

To search for other technical reports published by ERDC, visit the ERDC online library at <http://acwc.sdp.sirsi.net/client/default>.

Modeling the Transport of Oil Particle Aggregates and Mixed Sediment in Surface Waters

Earl Hayter
U.S. Army Engineer Research and Development Center
Environmental Laboratory
3909 Halls Ferry Road
Vicksburg, MS 39180-6199

Richard McCulloch and Todd Redder
LimnoTech, Inc.
501 Avis Drive
Ann Arbor, MI 48108

Michel Boufadel
New Jersey Institute of Technology
Center for Natural Resources Development and Protection
3909 323 MLK Blvd.
Newark, NJ 07102-1824

Rex Johnson
Global Remediation Technologies, Inc.
1102 Cass Steet
Traverse City, MI 49684

Faith Fitzpatrick
USGS WI Water Science Center
8505 Research Way
Middleton, WI 53562

Letter Report
Approved for public release; distribution is unlimited.

**Prepared for: U.S. Environmental Protection Agency, Region 5
Chicago, IL 60604-3590**

Abstract

The U.S. Army Engineer Research and Development Center (ERDC) worked with EPA Region 5, the USGS, the University of Illinois, and LimnoTech, Inc. on developing surface water hydrodynamic and transport models to simulate the transport of sediment and submerged oil in the Kalamazoo River, MI. The submerged oil present in the bottom sediments at different locations along a 38-mile reach of the river was released during one of the largest freshwater oil spills in North America. The spill occurred in July 2010 when the Enbridge Line 6B pipeline burst, releasing diluted bitumen into the Kalamazoo River downstream of Marshall, MI. Most of the floating oil was recovered quickly using conventional methods. However, the remaining oil mixed with river sediment, submerged, and deposited along 38 miles of the river. This necessitated the development and implementation of new approaches for detection and recovery for both submerged oil and oiled sediment as well the development of specialized transport models to more accurately predict the transport and fate of the residual oil and its association with bed sediments.

This report describes the modifications made to **LimnoTech's EFDC model** that includes the SEDZLJ sediment bed model. The oiled sediment, in the form of oil particle aggregates (OPA), was simulated as distinct particles from the mixed sediment particles represented in SEDZLJ. The changes made to EFDC and SEDZLJ to be able to represent the transport of both sediment and OPA were the following: 1) A separate transport module for the OPA was added to EFDC. 2) The percentages of OPA types present in the sediment bed along the modeled reach were determined and incorporated into a modified version of the SEDLZJ layered bed model. The modifications added the ability to represent a specified number of sediment size classes as well as a specified number of OPA classes or types. 3) The mass balance routines in EFDC were modified to calculate time- and space-averaged mass balances of the simulated classes of OPA.

Also presented are the unverified results from a simulation of sediment and OPA transport during a 13-day period in October-November 2011. Five size classes of sediment and three OPA classes were used in this modeling. The results show the change in the mass of the simulated OPA classes in the surface bed layer over the 13-day period as well as time series of concentrations of suspended OPA classes at three locations along the 38 miles. The simplified OPA transport module developed in this study is viewed as a first generation model, upon which more advanced modeling algorithms of OPA formation, transport, deposition, resuspension and potentially breakup can be built during future studies.

Contents

- 1 Introduction1**
 - Background..... 1**
 - Study Goal..... 1**
 - Study Tasks..... 1**

- 2 OPA Transport Module4**
 - Properties of OPAs 4**
 - Description of the OPA Transport Module.....6**

- 3 OPA and Sediment Transport Modeling10**
 - Description of the SEDZLJ Sediment Bed Model10**
 - Incorporation of the OPA transport Module into EFDC and SEDZLJ..... 17**
 - Model Testing..... 21**
 - Modeling Results..... 22**

- 4 Conclusions and Recommendation.....37**

- References.....38**

- Appendix A - Process of overlaying oiling categories onto SEDZLJ
bed layers for EFDC modeling.....41**

Figures and Tables

Figures

Figure 1-1. Location map of the Kalamazoo River affected by the July 2010 Enbridge Line6B oil spill (after Fitzpatrick *et al.* 2015)..... 2

Figure 2-1. Types of OPAs: (A) single and multiple droplet aggregate; (B) solid aggregate of large, elongated oil mass with interior particles (dashed blue circles); and (C) flake aggregate of thin membranes of clay aggregates that incorporate oil. Blue color represents particles and yellow represents oil. (after Fitzpatrick *et al.*, 2015)..... 5

Figure 3-1. Sediment transport processes simulated in SEDZLJ12

Figure 3-2. Schematic of Multi-Bed Layer Model used in SEDZLJ along with example Erosion Rate versus Depth Curves15

Figure 3-3. Schematic of Active Layer used in SEDZLJ15

Figure 3-4. Total OPA Concentration Time Series at the Specified Three Locations23

Figure 3-5. Longitudinal Total OPA concentrations at the end of the 13-day simulation25

Figure 3-6a. Longitudinal OPA Concentrations for Type 1 OPA at the end of the 13-day simulation26

Figure 3-6b. Longitudinal OPA Concentrations for Type 2 OPA at the end of the 13-day simulation27

Figure 3-6c. Longitudinal OPA Concentrations for Type 3 OPA at the end of the 13-day simulation28

Figure 3-7a. Percentages of OPA Type 1 in Bed Layer 2 at the beginning of the 13-day simulation29

Figure 3-7b. Percentages of OPA Type 1 in Bed Layer 2 at the end of the 13-day simulation30

Figure 3-8a. Percentages of OPA Type 2 in Bed Layer 2 at the beginning of the 13-day simulation31

Figure 3-8b. Percentages of OPA Type 2 in Bed Layer 2 at the end of the 13-day simulation32

Figure 3-9a. Percentages of OPA Type 3 in Bed Layer 2 at the beginning of the 13-day simulation33

Figure 3-9b. Percentages of OPA Type 3 in Bed Layer 2 at the end of the 13-day simulation34

Figure 3-10. Change in Bed Elevation over the 13-day simulation35

Figure 3-11. Change in Bed Elevation from -0.1 to 0.1 m over the 13-day simulation36

Tables

Table 2-1. OPA Properties..... 7

Table 2-2. OPA Percentages in Layered Sediment Bed 8

Table 3-1. OPA.INP Input File19

Table 3-2. OPA_PERCENTAGES.prn Input File.....20

Table A-1. Oil Concentrations in the Five Sediment Bed Layers.....42

Table A-2. Oil and OPA Percentages used for the Five Sediment Bed Layers.....43

1 Introduction

Background

The U.S. Army Engineer Research and Development Center (ERDC), has been working with EPA Region 5, the USGS, the University of Illinois, and LimnoTech, Inc. on developing surface water hydrodynamic and transport models to simulate the transport of sediment and submerged oil in the Kalamazoo River, MI. The submerged oil present in the bottom sediments at different locations along a 38-mile reach of the river was released during one of the largest freshwater oil spills in North America (see Figure 1-1). The spill occurred in July 2010 when the Enbridge Line 6B pipeline burst, releasing diluted bitumen into the Kalamazoo River downstream of Marshall, MI. As described elsewhere (Fitzpatrick *et al.* 2015), the spill occurred during a flood with a 4 percent exceedance probability (Hoard *et al.*, 2010). Most of the floating oil was recovered quickly using conventional methods such as surface containment, absorbent boom, vacuum trucks, and drum skimmers (Dollhopf *et al.*, 2014). However, the remaining oil mixed with river sediment, submerged, and deposited along 38 miles of the river. This necessitated the development and implementation of new approaches for detection and recovery for both submerged oil and oiled sediment (Dollhopf *et al.*, 2014). These included the development of hydrodynamic and specialized transport models to more accurately predict the transport and fate of the residual oil and its association with bed sediments.

Study Goals

Develop a new transport model to simulate the resuspension, transport and fate of the residual oil and associated sediments located mostly in depositional zones along the 38-mile reach of the Kalamazoo River, and apply it to simulate the transport of these constituents during selected periods with varying flow conditions.

Study Tasks

Task 1. Develop a Conceptual Site Model for the Residual Oil

Using existing data as well as data collected and experiments performed

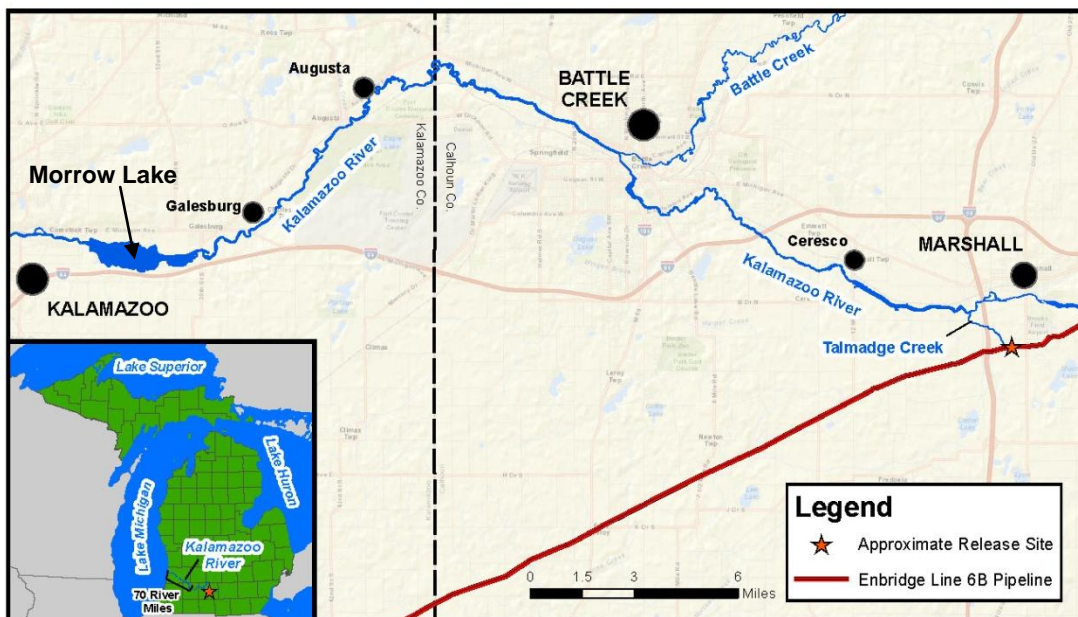


Figure 1-1. Location map of the Kalamazoo River affected by the July 2010 Enbridge Line 6B oil spill (after Fitzpatrick *et al.* 2015).

during the study performed for EPA, a conceptual model for the aggregate structure formed by residual oil and sediments was developed. This is described in Section 2.

Task 2. Develop Transport Module for the Residual Oil

The conceptual model was used to develop a transport module capable of simulating the resuspension and subsequent transport of the oil-sediment aggregate structure when linked to a hydrodynamic model. This module is described in Section 2.

Task 3. Integrate the Residual Oil Transport Module into the EFDC Model

The new residual oil transport module was integrated into the hydrodynamic module in EFDC as well as into the SEDZLJ sediment bed model in EFDC. The model user selects if sediment transport and residual oil transport or just sediment transport are simulated.

Task 4. Test the New Version of EFDC

The following numerical tests were performed in verifying the new version of EFDC: 1) the ability of the model to conserve both sediment and residual oil mass was evaluated; and 2) the new model was run to simulate

only sediment transport and the results were compared with those from **LimnoTech's original model to insure that adding the new residual oil transport module did not change simulated sediment transport results.**

Task 5. Simulate Transport of Sediments and Residual Oil Using the New Version of EFDC

The new model was used to simulate the transport of both mixed sediment and residual oil over a 13-day high baseflow period in October 2011. The results from this simulation are described in Section 3.

2 OPA Transport Module

Properties of OPAs

During the study performed for EPA, the physical properties of the submerged residual oil in the sediment, including its persistence in the environment, were studied. In the initial sediment transport modeling that Tetra Tech, Inc. performed for Enbridge Oil, they assumed that the residual oil was transported along with the silt-size sediment particles. However, visual examinations of released globs of the residual oil caused by agitation of sediment during poling assessments, observations of oil globs in sediment cores, and ultraviolet epi-fluorescence microscopy of oil and sediment mixtures revealed that the oiled sediment was in the form of oil-mineral aggregates, similar to those that have been found to form in marine environments (Lee, 2002; Lee *et al.*, 2011; Lee *et al.*, 2012; Dollhopf *et al.*, 2014). These oil-mineral aggregates were renamed oil-particle aggregates (OPAs) since the particulate matter in the sediment in the Kalamazoo River is composed of both organic and inorganic particles. The specific properties of OPAs that were investigated included the structure, i.e., shape and arrangement, of OPAs (Fig. 2-1), oil droplet size, oil density, number of oil droplets in an OPA, size and density of OPAs, and the settling velocity and critical shear stress to resuspend OPAs. A brief summary of these laboratory studies is given below.

Waterman and Garcia (2014) describe several laboratory experiments and flume tests that were performed at the University of Illinois Ven Te Chow Hydrosystems Laboratory to specifically quantify the weathering characteristics of the dilbit and the properties of OPAs formed by its subsequent mixing with sediments in the Kalamazoo River. These tests are summarized below.

- Laboratory tests were performed in which the diluent was weathered to promote removal of the diluent component while measuring oil mass loss, and oil density and viscosity over the range of temperatures found in the Kalamazoo River. In these tests the weathered dilbit remained positively buoyant at room temperatures which was also found by Belore (2010). However, a recent study by

King et al., 2014) reported negatively buoyant dilbit in freshwater after weathering.

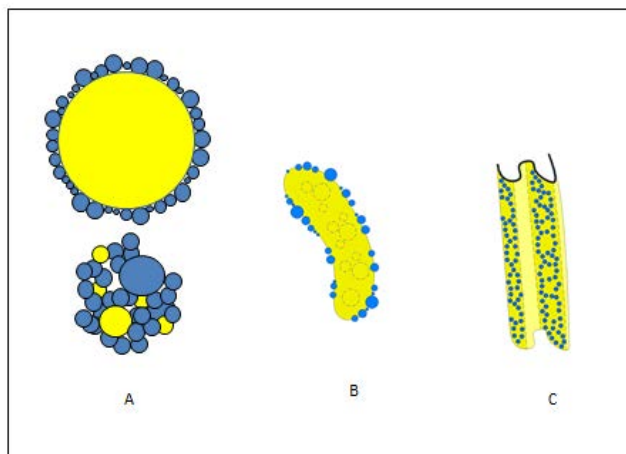


Figure 2-1. Types of OPAs: (A) single and multiple droplet aggregate; (B) solid aggregate of large, elongated oil mass with interior particles (dashed blue circles); and (C) flake aggregate of thin membranes of clay aggregates that incorporate oil. Blue color represents particles and yellow represents oil. (after Fitzpatrick *et al.*, 2015)

- The size distributions of the OPAs were tested using an orbital shaker operated at a range of mixing energies. The OPA sizes were found to be functions of the oil viscosity and the amount of turbulence.
- To study the formation of OPAs, weathered bitumen was mixed in the shaker with sediment from the Kalamazoo River, with the mixing energy and time, sediment types and concentrations varied during the tests.
- Photography was used to measure the size of the OPAs and a Laser In-Situ Scattering and Transmissiometry (LISST) instrument was used to measure the small OPAs.
- Examination of OPAs under an ultraviolet epi-fluorescence microscope showed that the OPAs were composed of irregular shaped aggregates of oil globules that ranged in size from about 10 to 100 μm and had particles less than about 10 μm attached to

them. The most common type of OPA that was observed was the single and multiple droplet aggregates (see Figure 2-1A).

- Annular flume experiments were performed to determine the critical bed shear stress for resuspension of the OPAs. In addition, a settling column was used to measure the settling velocities of OPAs.

Description of the OPA Transport Module

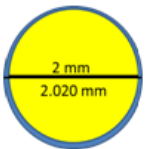
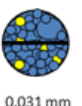
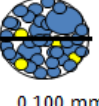
The basic framework – including assumptions incorporated into the OPA transport model - for representing the transport of OPAs in EFDC is described below.

- The formation and disaggregation of OPAs are not simulated in this transport module. Thus, unless OPAs are simulated to be transported out of the model domain across the downstream boundary, the types and mass of OPAs specified in the initial conditions does not change during the simulation.
- The different types of OPAs are represented as separate particle size classes that exist at the start of the model simulation, *i.e.*, initial conditions, in the multi-layers sediment bed model. Specifically, they represent the oiling conditions in the Kalamazoo River in 2012.
- Data from the OPA studies described previously and from Lee *et al.* (2012), and from onsite observations from poling assessments and cores were used to determine that three classes of OPAs needed to be included in the transport module. The three OPA classes are used to represent the multiple sizes and structures of oil globules and OPAs in the riverbed.
- The three OPA classes range from a large 2 mm single oil globule with a 10 μm silt coating to more complex OPAs with multiple smaller globules and OPA diameters of 31 μm and 100 μm (see Table 2-1).
- Densities of these OPA classes range from just greater than the density of freshwater for the large oil globule with silt coating

(1.034 g/cm³) to somewhat heavier and close to the density of organic particles for the Type 3 OPAs (1.511 g/cm³) (see Table 2-1).

- Calculated OPA settling velocities range from 0.2 to 28 mm/s, depending on the amount of oil relative to the size of the aggregate (see Table 2-1). These were calculated using the methodology by Zhao *et al.* (2014). The last two lines in this table (with the red highlighting) represent an example case with typical values used for the oil and OPA concentrations.

Table 2-1 OPA Properties

			
	Type 1 OPA (large droplet with silt coating)	Type 2 OPA (silt aggregate with smaller oil droplets)	Type 3 OPA (larger silt aggregate with small oil droplets)
OPA Assumptions and calculations			
Oil droplet diameter (mm)	2.00	0.02	0.05
Particulate diameter (mm)	0.01	variable	variable
OPA diameter (mm)	2.020	0.031	0.10
Number of oil droplets per OPA	1.0	2.0	4.0
% Mineral particulate in OPA	100.0	75.0	75.0
% Organic particulate in OPA	0.0	25.0	25.0
OPA Porosity (%)	0.0	20.0	20.0
Oil droplet volume in OPA (sphere) (cm ³)	4.189E-03	8.378E-09	2.618E-07
OPA total volume (sphere) (cm ³)	4.316E-03	1.248E-08	4.189E-07
OPA particulate volume (cm ³)	1.269E-04	4.101E-09	1.571E-07
oil mass per OPA (g)	4.126E-03	8.252E-09	2.579E-07
particulate mass per OPA (g)	3.364E-04	9.792E-09	3.750E-07
oil + particulate OPA total mass (g)	4.462E-03	1.804E-08	6.329E-07
Mass (oil) / Mass (OPA) (%)	92.46	45.73	40.74
Mass (oil) / Mass (OPA) (mg/kg)	924624.2	457331.1	407445.7
OPA specific gravity (SG) - assumes spherical aggregates	1.03	1.45	1.51
Stokes Settling velocity (mm/s)	75.54	0.23	2.78
Settling velocity (mm/s) - Zhao et al. (2014)	27.69	0.23	2.78
Oil concentration [Mass (oil) / Mass (substrate)] (mg/kg)	144.4	144.4	225.6
OPA concentration [Mass (OPA) / Mass (substrate)] (mg/kg)	156.2	315.8	553.8

- The layered sediment bed SEDZLJ required data on the mass fraction of each OPA size class in each layer for each of the different types of sediment “cores” or types. In this context, a sediment core consists of the bulk density, grain size distribution, and erosion rate in each bed layer. The Kalamazoo River streambed from the 2012 Enbridge model was updated with SEDFLUME core data to obtain

layer properties, and then further overlaid with 2012 oiled areas of the river to identify streambed locations that were in a moderate-to-heavy oiled or none-to-light oiled areas. The OPA mass fractions for layers in each oiling category were estimated from the measured oil concentrations, plus the estimated initial proportions of the OPA types and the respective mass per OPA (as illustrated in the last three rows of Table 2-1). The OPA percent mass fractions based on streambed measured oil concentrations for the Kalamazoo River are given in Table 2-2.

Table 2-2 OPA Mass Fractions (%) in Layered Sediment Bed

OPA distributions by vertical layering and oiling category	Type 1 OPA (%)	Type 2 OPA (%)	Type 3 OPA (%)
Heavy/Moderate Top layer (0-2 cm)	0.01258	0.02544	0.02855
Heavy/Moderate Layer 2 (2-5 cm)	0.00782	0.01582	0.01775
Heavy/Moderate Layer 3 (5-10 cm)	0.00761	0.01538	0.01726
Heavy/Moderate Layer 4 (10-18 cm)	0.00782	0.01582	0.01775
Heavy/Moderate Layer 5 (18-30 cm)	0.00620	0.01254	0.01407
Light/None Top layer (0-2 cm)	0.00856	0.01731	0.01943
Light/None Layer 2 (2-5 cm)	0.00467	0.00944	0.01059
Light/None Layer 3 (5-10 cm)	0.00472	0.00955	0.01072
Light/None Layer 4 (10-18 cm)	0.00461	0.00933	0.01047
Light/None Layer 5 (18-30 cm)	0.00397	0.00802	0.00900

- OPAs are assumed to be transported only in suspension and not as bedload.
- Details of the integration of the OPA transport module into the SEDZLJ sediment bed model are described in Section 3. The OPA transport module solves the multi-dimensional advective – dispersive transport equation given by Equation 3-1, with C_i = mass concentration of the i^{th} class of OPAs. The EFDC model user selects whether to activate the OPA transport module or not during setup of the model. The value of S_i = source/sink term in this equation is calculated by the SEDZLJ sediment bed model. The solution of this transport equation gives the spatially and temporally varying water column mass concentrations of the three OPA particle types.

The simplified OPA transport module developed in this study is viewed as a first generation model, upon which more advanced modeling algorithms of OPA formation, transport, deposition, resuspension and potentially breakup can be built during future studies.

3 OPA and Sediment Transport Modeling

Prior to describing the incorporation of the OPA transport module into EFDC, the SEDZLJ sediment bed model is described below. In particular, an understanding of the multiple bed layer SEDZLJ model is essential to understanding how the OPA transport module was linked to both the transport module in EFDC and to SEDZLJ.

Description of the SEDZLJ Sediment Bed Model

The sediment transport model in EFDC is the SEDZLJ sediment transport model (Jones and Lick, 2001; James *et al.*, 2010). SEDZLJ is dynamically linked to EFDC in that the hydrodynamics and sediment transport modules are run during each model time step. A description of this sediment transport model is given next.

Suspended Load Transport of Sediment

The EFDC hydrodynamic module simulates the transport of each of the sediment classes to determine the suspension concentration for each size class in every water column layer in each grid cell. The transport of suspended sediment is determined through the solution of the following 3D advective-dispersive transport equation for each of the sediment size classes that is used in the model:

$$\frac{\partial C_i}{\partial t} + \frac{\partial u C_i}{\partial x} + \frac{\partial v C_i}{\partial y} + \frac{\partial (w - W_{Si}) C_i}{\partial z} = \frac{\partial}{\partial x} \left(K_H \frac{\partial C_i}{\partial x} \right) + \frac{\partial}{\partial y} \left(K_H \frac{\partial C_i}{\partial y} \right) + \frac{\partial}{\partial z} \left(K_V \frac{\partial C_i}{\partial z} \right) + S_i \quad (3-1)$$

where C_i = concentration of i th size class of suspended sediment, (u, v, w) = velocities in the (x, y, z) directions, t = time, W_{Si} = settling velocity of i th sediment size class, K_H = horizontal turbulent eddy diffusivity coefficient, K_V = vertical turbulent eddy diffusivity coefficient, and S_i = source/sink term for the i th sediment size class that accounts for erosion/deposition.

The settling velocities for noncohesive sediments are calculated in SEDZLJ using the following equation (Cheng, 1997):

$$W_s = \frac{\mu}{d} \left(\sqrt{25 + 1.2d_*^2} - 5 \right)^3 \quad (3-2)$$

where μ = dynamic viscosity of water; d = sediment diameter; and d^* = non-dimensional particle diameter given by:

$$d_* = d \left[(\rho_s / \rho_w - 1) g / \nu^2 \right]^{1/3} \quad (3-3)$$

where ρ_w = water density, ρ_s = sediment particle density, g = acceleration due to gravity, and ν = **kinematic fluid viscosity**. **Cheng's formula is based on measured settling speeds of real sediments. As a result it produces slower settling speeds than those given by Stokes' Law because real sediments have irregular shapes and thus a greater hydrodynamic resistance than perfect spheres as assumed in Stokes' law.**

The erosion and deposition of each of the sediment size classes, i.e., the source/sink term in the 3D transport equation given above, and the subsequent change in the composition and thickness of the sediment bed in each grid cell are calculated by SEDZLJ at each time step.

Description of SEDZLJ

SEDZLJ is an advanced sediment bed model that represents the dynamic processes of erosion, bedload transport, bed sorting, armoring, consolidation of fine-grain sediment dominated sediment beds, settling of flocculated cohesive sediment, settling of individual noncohesive sediment particles, and deposition. An active layer formulation is used to describe sediment bed interactions during simultaneous erosion and deposition. The active layer facilitates coarsening during the bed armoring process. The SEDZLJ model was designed to directly use the results obtained from a SEDFLUME study. A description of SEDFLUME is available at <http://chl.erdc.usace.army.mil/CHL.aspx?p=s&a=ARTICLES:630>. SEDFLUME is a straight, closed conduit rectangular cross-section flume in which detailed measurements of critical shear stress of erosion and erosion rate as a function of sediment depth are made using sediment cores (dominated by cohesive or mixed sediments) that are collected at the site to be modeled (McNeil *et al.*, 1996). However, when SEDFLUME results are not available, it is possible to use a combination of literature values for these parameters as well as the results of SEDFLUME tests performed at other similar sites. In this case, a detailed sensitivity analysis should be performed to assist in quantifying the uncertainty that results from the use of these non-site specific erosion parameters.

Figure 3-1 shows the simulated sediment transport processes in SEDZLJ. In this figure, U = near bed flow velocity, C = near bed sediment concentration, δ_{bl} = thickness of layer in which bedload transport occurs, U_{bl} = average bedload transport velocity, D_{bl} = sediment deposition rate for the sediment being transported as bedload, E_{bl} = sediment erosion rate for the sediment being transported as bedload, E_{sus} = sediment erosion rate for the sediment that is eroded and entrained into suspension, and D_{sus} = sediment deposition rate for suspended sediment. Specific capabilities of SEDZLJ are listed below.

- Whereas a hydrodynamic model is calibrated to account for the total bed shear stress, which is the sum of the form drag due to bed forms and other large-scale physical features (*e.g.*, boulders) and the skin friction (also called the surface friction), the relevant component of the bed shear stress to use in predicting sediment resuspension and deposition is the skin friction. The skin friction is calculated in SEDZLJ as a function of the near-bed current velocity and the effective bed roughness. The latter can be specified in SEDZLJ as a linear function of the mean particle diameter in the active layer, or it can also be specified as a constant as it was for this modeling study.
- Multiple size classes of both fine-grain (*i.e.*, cohesive) and noncohesive sediments can be represented in the sediment bed. This capability is necessary in order to simulate coarsening and subsequent armoring of the surficial sediment bed surface during high flow events.

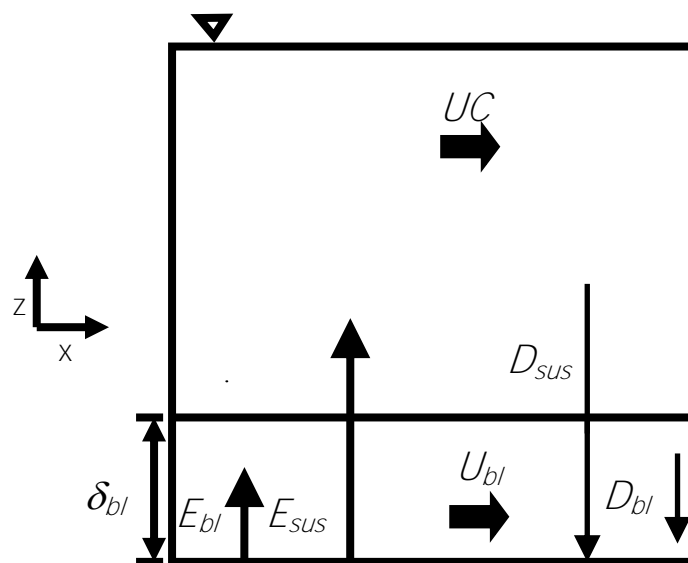


Figure 3-1 Sediment transport processes simulated in SEDZLJ

- To correctly represent the processes of erosion and deposition, the sediment bed in SEDZLJ can be divided into multiple layers, some of which are used to represent the existing sediment bed and others that are used to represent new bed layers that form due to deposition during model simulations. Figure 3-2 shows a generic schematic diagram of this multiple bed layer structure. The graph on the right hand side of this figure shows the variation in the measured gross erosion rate (in units of **cm/s**) with depth into the sediment bed as a function of the applied skin friction. A SEDFLUME study (as is described in the next section) is normally used to measure these erosion rates.
- Erosion from both cohesive and non-cohesive beds is affected by bed armoring, which is a process that limits the amount of bed erosion that occurs during a high-flow event. Bed armoring occurs in a bed that contains a range of particle sizes (*e.g.*, clay, silt, sand). During a high-flow event when erosion is occurring, finer particles (*i.e.*, clay and silt, and fine sand) tend to be eroded at a faster rate than that of coarser particles (*i.e.*, medium to coarse sand). The differences in erosion rates of the various sediment particle sizes creates a thin layer at the surface of the sediment bed, referred to as the active layer, that is depleted of finer particles and enriched with coarser particles. This depletion-enrichment process can lead to bed armoring, where the active layer is primarily composed of coarse particles that have limited mobility. Deposition of coarser particles transported from upstream can also lead to bed armoring. The multiple bed layer model in SEDZLJ accounts for the exchange of sediment through and the change in composition of this active layer. The thickness of the active layer, T_a , is calculated as the time varying function (shown in Equation 3-4) of the mean sediment particle diameter in the active layer, d_{50} , the critical shear stress for resuspension corresponding to the mean particle diameter τ_{cr} , and the bed shear stress τ (Van Niekerk *et al.* 1992).

$$T_a = 2d_{50} \frac{\tau}{\tau_{cr}} \quad (3-4)$$

Figure 3-3 shows a schematic of the active layer at the top of the six bed layer model used in SEDZLJ for this modeling study. Sediment deposits during a model run are put in the second layer, and layers 3 – 6 represent the original (*i.e.*, parent) four-layer sediment bed.

- SEDZLJ can simulate overburden-induced consolidation of cohesive sediments. An algorithm that simulates the process of primary consolidation, which is caused by the expulsion of pore water from the sediment, of a fine-grained, *i.e.*, cohesive, dominated sediment bed is included in SEDZLJ. The consolidation algorithm in SEDZLJ accounts for the following changes in two important bed parameters: 1) increase in bed bulk density with time due to the expulsion of pore water, and 2) increase in the bed shear strength (also referred to as the critical shear stress for resuspension) with time. The latter parameter is the minimum value of the bed shear stress at which measurable resuspension of cohesive sediment occurs. As such, the process of consolidation typically results in reduced erosion for a given excess bed shear stress (defined as the difference between the bed shear stress and bed shear strength) due to the increase in the bed shear strength. In addition, the increase in bulk density needs to be represented to accurately account for the mass of sediment (per unit bed area) that resuspends when the bed surface is subjected to a flow-induced excess bed shear stress. Models that represent primary consolidation range from empirical equations that approximate the increases in bed bulk density and critical shear stress for resuspension due to porewater expulsion (Sanford, 2008) to finite difference models that solve the non-linear finite strain consolidation equation that governs primary consolidation in saturated porous media (Arega and Hayter, 2008). Consolidation was not simulated in this modeling study due to lack of data to define the empirical relationships between the increase of bed shear strength and bulk density with time.

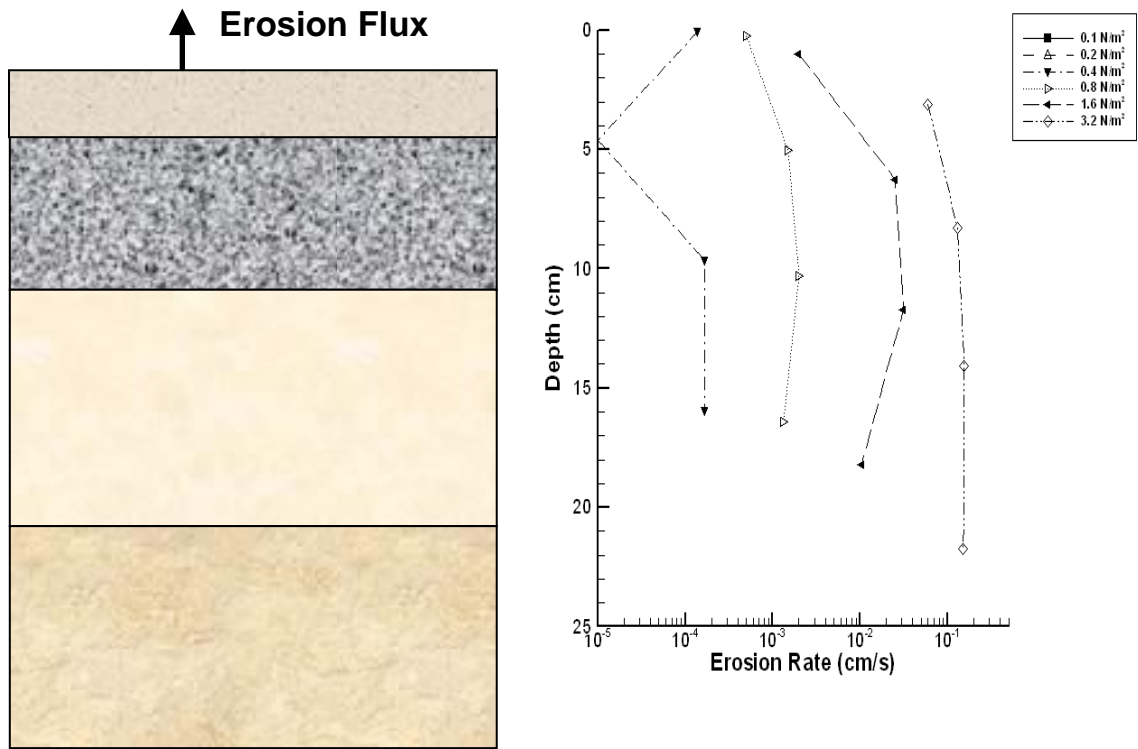


Figure 3-2 Schematic of Multi-Bed Layer Model used in SEDZLJ along with example Erosion Rate versus Depth Curves.

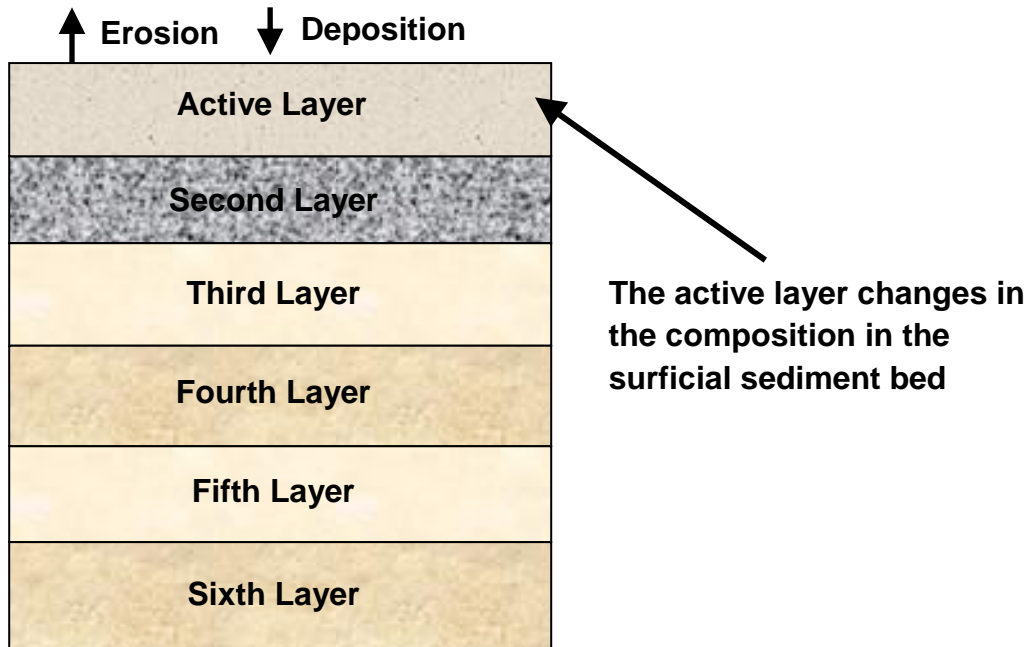


Figure 3-3 Schematic of Active Layer used in SEDZLJ

An empirical-based consolidation algorithm is included in SEDZLJ. Simulation of consolidation requires performing specialized consolidation experiments to quantify the rate of consolidation. These experiments were not conducted as a component of this modeling study, and as such, consolidation was not simulated.

- SEDZLJ contains a morphologic algorithm that, when enabled by the model user, will adjust the bed elevation to account for erosion and deposition of sediment.
- SEDZLJ accounts for the effect of bed slope on erosion rates and bedload transport. The bed slopes in both the x- and y-directions are calculated, and scaling factors are applied to the bed shear stress, erosion rate, and bedload transport equations. A maximum adverse bed slope is specified that prevents bedload transport from occurring up too steep a slope.

Bedload Transport of Noncohesive Sediment

The approach used by Van Rijn (1984) to simulate bedload transport is used in SEDZLJ. The 2D mass balance equation for the concentration of sediment moving as bedload is given by:

$$\frac{\partial(\delta_{bl}C_b)}{\partial t} = \frac{\partial q_{b,x}}{\partial x} + \frac{\partial q_{b,y}}{\partial y} + Q_b \quad (3-4)$$

where δ_{bl} = bedload thickness; C_b = bedload concentration; $q_{b,x}$ and $q_{b,y}$ = x- and y-components of the bedload sediment flux, respectively; and Q_b = sediment flux from the bed. Van Rijn (1984) gives the following equation for the thickness of the layer in which bedload is occurring:

$$\delta_{bl} = 0.3dd_*^{0.7}(\Delta\tau)^{0.5} \quad (3-5)$$

where $\Delta\tau = \tau_b - \tau_{ce}$; τ_b = bed shear stress, and τ_{ce} = critical shear stress for erosion.

The bedload fluxes in the x- and y-directions are given by:

$$q_{b,x} = \delta_{bl}u_{b,x}C_b$$

$$q_{b,y} = \delta_{bl}u_{b,y}C_b$$

where $u_{b,x}$ and $u_{b,y}$ = x - and y -components of the bedload velocity, u_b , which van Rijn (1984) gave as

$$u_b = 1.5\tau_*^{0.6} \left[\left(\frac{\rho_s}{\rho_w} - 1 \right) gd \right]^{0.5} \quad (3-6)$$

with the dimensionless parameter τ_* given as

$$\tau_* = \frac{\tau_b - \tau_{ce}}{\tau_{ce}} \quad (3-7)$$

The x - and y -components of u_b are calculated as the vector projections of the CH3D Cartesian velocity components u and v .

The sediment flux from the bed due to bedload, Q_b , is equal to

$$Q_b = E_b - D_b \quad (3-8)$$

where E_b is the erosion of sediment into bedload, and D_b is the deposition of sediment from bedload onto the sediment bed.

Incorporation of the OPA Transport Module into EFDC and SEDZLJ

As described in Section 2, an additional transport module was added to EFDC to simulate the transport of OPAs. The OPA transport module is activated by the model user in the C6 Card in the EFDC.INP file, which is the master input file for EFDC. This transport module solves the multi-dimensional advective – dispersive transport equation given by Equation 3-1, where C_i = mass concentration of the i^{th} class of OPAs. The solution of this equation gives the spatially and temporally varying water column mass concentrations of the three OPA particle types.

The value of S_i = source/sink term in Equation 3-1, which is equal to the gross erosion rate minus the deposition rate of the OPA particles in each grid cell, is calculated by the SEDZLJ sediment bed model. Details of the integration of the OPA transport module into the SEDZLJ sediment bed model are described next.

When the OPA transport module is activated, the SEDZLJ bed model reads in the **OPA.INP** input file (see Table 3-1). The main parameters read from this file include NOPA = number of OPA classes; the D50, settling velocities and specific gravities of the NOPA classes; the initial suspension

concentration of the NOPA classes; at NOPASER = number of time series of OPA concentrations specified at the locations of inflow into the model domain. As seen in this table, there are two time series used, and there are 13 locations, i.e., grid cells, where water flows into the model domain. When NOPASER is greater than zero, then the **OPASER.INP** input file is read. This contains the NOPASER number of time series.

Another input file that is read when NOPA is greater than zero is **Oil_categories.prn**. This specifies for every grid cell whether the oiling in the sediment bed in that cell is “Light/None” or “Heavy/Moderate”. The process of overlaying these oiling categories onto the SEDZLJ bed layers is described in Appendix A.

The file **OPA_PERCENTAGES.prn** is also read. This file is shown in Table 3-2. Depending on if a particular grid cell is classified as being “Light/None” or “Heavy/Moderate”, the percentages for the three OPA classes (types) are given in the three columns in this table. The first row of values is for Layer 3 (top 2 cm in the parent sediment bed), the second row is for Layer 4 (2-5 cm from the top of the parent sediment bed), the third row is for Layer 5 (5-18 cm), and the fourth row is for Layer 6 (18-30 cm). The percentages given in this table are the same as those given in Table 2-2, except that data for layers 3 and 4 from Table 2-2 were consolidated into a single layer for the model.

Table 3-1 OPA.INP Input File

```

*   OPA.INP
*
*   NOPA:      number of OPA classes
*   IOPAAP:    OPA approach
*   1          aggregate (only option working at present)
*   2          oil sorbed to solids (either organic or inorganic)
*
*   NOPA      IOPAAP
*   3         1
*   D50 ( $\mu\text{m}$ )  SETTLING VELOCITY (cm/s)  SSGOPA
*   2020.0      2.769          1.034
*   31.0        0.023          1.446
*   100.0       0.278          1.511
*   INITIAL SUSPENDED CONCENTRATION (mg/L)
*   0.0
*   0.0
*   0.0
*   NOPASER: NUMBER OF OPA CONCENTRATION TIME SERIES
*   EACH TIME SERIES MUST HAVE DATA FOR NOPA OPAs
*   NOPASER
*   2
C24  IQS  JQS  NOPAQ  QSFACTOR
2177 39   1     1.0   ! Upstream Boundary Condition
2177 40   1     1.0   ! Upstream Boundary Condition
2177 41   1     1.0   ! Upstream Boundary Condition
2177 42   1     1.0   ! Upstream Boundary Condition
1412 44   1     1.0   ! Battle Creek
1412 45   1     1.0   ! Battle Creek
2150 35   2     1.0   ! Talmadge Creek
2133 47   1     1.0   ! Bear Creek
1554 35   1     1.0   ! Harper & Minges Brook
704  51   1     1.0   ! Augusta Creek
1208 46   1     1.0   ! Wabascon Creek
1094 47   1     1.0   ! Seven Mile Creek
448  50   1     1.0   ! Gull Creek

```

Table 3-2 OPA_PERCENTAGES.prn Input File

```

!      Light/none - for layers 3–6: Types 1,2,3 are in the 1st, 2nd, 3rd columns
0.0086      0.0173      0.0194
0.0047      0.0095      0.0106
0.0046      0.0093      0.0105
0.0040      0.0080      0.0090
!      Heavy/moderate - for layers 3–6: Types 1,2,3 are in the 1st, 2nd, 3rd cols
0.0126      0.0254      0.0286
0.0076      0.0155      0.0175
0.0078      0.0158      0.0178
0.0062      0.0125      0.0141
    
```

Next, the SEDZLJ bed model reads in a modified version of the **sdf_main.inp** input file. In this file the following two lines of data were modified by adding the critical shear stress for erosion and the critical shear stress for suspension for the three OPA types to the end of each line of data. That is, the critical shear stresses for erosion of OPA Type 1, 2, and 3 were all set equal to 0.5 dynes/cm². The two critical shear values are the same for the OPA classes since they are assumed to be transported only in suspension and not as bedload. The first five values in these two lines are the critical shear stresses for the five sediment size classes used in the sediment transport modeling (LimnoTech 2014).

```

# Critical Shear for Suspension TCRDPS(K) [dynes/cm^2] #
0.50 0.50 1.00 1.50 8.2 0.50 0.50 0.50
# Critical Shear for Erosion TAUCRS(K) [dynes/cm^2] #
0.50 0.50 1.00 1.50 8.2 0.50 0.50 0.50
    
```

In the **sdf_cores.inp** file, the percentages of the specified number of sediment size classes in each bed layer are read for all the different sediment cores. When NOPA > 0, then those percentages are adjusted to account for the small mass percentages of the different types of OPAs given in the OPA_PERCENTAGES.prn file. This is done by summing the percentages of the three OPA types and subtracting that total from the percentage of the largest sediment size class present in the bed layers in each grid cell. This insures that the total percentage of sediment and OPAs in each bed layer equals 100 percent.

When the bed shear stress exceeds the critical shear stress for erosion of the top bed layer, a calculated thickness of the bed surface is eroded. The mass of the sediment and OPAs in that layer is added to the water column in that grid cell, and the subsequent advection, dispersion, and settling of

the eroded sediment and OPAs are calculated by the sediment and OPA transport modules. Since the EFDC model of the 38-mile reach of the Kalamazoo River is being run in the depth-averaged mode, the deposition rate of suspended OPAs is calculated as the product of the concentration of OPA, the settling velocity (given in OPA.INP), and the probability of deposition.

Model Testing

Results from a SEDFLUME study (Perkey *et al.*, 2014) and from *in situ* flume tests (Waterman *et al.*, 2014) were used, along with other field data, for characterizing the mixed sediment properties in the modified EFDC model. LimnoTech (2014) describes the methodology for using the **SEDFLUME data and other data to develop six sediment “cores”** (and the SEDZLJ input files) that were used to specify these properties in each grid cell. The 13-day high baseflow simulation from Oct 28 - Nov 9, 2011 that LimnoTech setup was used to test the modified model. The following numerical tests were performed to verify the new version of EFDC: 1) the ability of the model to conserve both sediment and residual oil mass was evaluated; and 2) the new model was run to simulate only sediment **transport and the results were compared with those from LimnoTech’s** original model to insure that adding the new residual oil transport module did not change simulated sediment transport results. The following are the results from these tests.

- Over the 13-day model run, 98 percent of the total mass of sediment and OPAs were conserved. Based on the extensive experience of the **authors’** in the use of EFDC over the past 15 years, this is an excellent result.
- The modified model was run with $NOPA=0$, *i.e.*, the OPA transport module inactivated, for the 13-day high baseflow simulation and the sediment transport results were compared with those obtained using **LimnoTech’s model. All the results were the same.**

These tests verified that the modified EFDC model correctly represents the transport of OPAs.

Modeling Results

Some results from the 13-day high baseflow simulation from Oct 28 - Nov 9, 2011 are presented in this section. This simulation started with a spun-up sediment bed. Figure 3-4 shows time series over the last 12 days of the simulation of the predicted discharge and total OPA concentrations at the following locations: a) Mile Post (MP) 9.25; b) MP 14.1; c) MP 18.1; and d) the 35th Street bridge. The first day of the 13-day simulation was not plotted so as not to show the effect of model start up. The simulated OPA concentration at the most downstream location (35th Street bridge) is seen to be the lowest. The numerous spikes seen in the OPA concentrations at all four locations over the last 12 days of the model run are caused by erosion of surficial sediment bed and entrainment of embedded OPAs into the water column. These results as well as results at other locations along the modeled reach of the river confirm that OPA was entrained at most non-impounded locations several times over the 13-day run.

Figure 3-5 shows the longitudinal profile of the total OPA concentration at the end of the 13-day model run. The impact of lower flow velocities in the backwater region upstream from dams on OPA concentrations was as expected, *e.g.*, the decrease in concentrations in the region immediately upstream from Ceresco Dam. Figures 3-6a,b,c show the same longitudinal profile for the three OPA types. Type 1 concentrations were the lowest, and Type 3 concentrations were just slightly higher than Type 2 during most of the 13-day simulation. In Figures 3-4 - 3-6, the decreasing OPA concentrations are due to deposition of the OPAs as they are advected downstream, and increases in OPA concentrations are due to erosion of the surficial sediment bed.

As an example of additional results obtained from the model run, the following describes results found in Morrow Lake. Figures 3-7a and 3-7b show the initial ($t = 0$) and final ($t = 13$ days) percentages of OPA Type 1 in bed layer 2, respectively, at the downstream end of the modeled reach (*i.e.*, Morrow Lake). Results in bed layer 2 are shown since, as previously noted, they show the sediment and OPAs that are simulated to deposit during the model run. Figures 3-8a and 3-8b show the initial ($t = 0$) and final ($t = 13$ days) percentages of OPA Type 2 in bed layer 2, and Figures 3-9a and 3-9b show the initial ($t = 0$) and final ($t = 13$ days) percentages of OPA Type

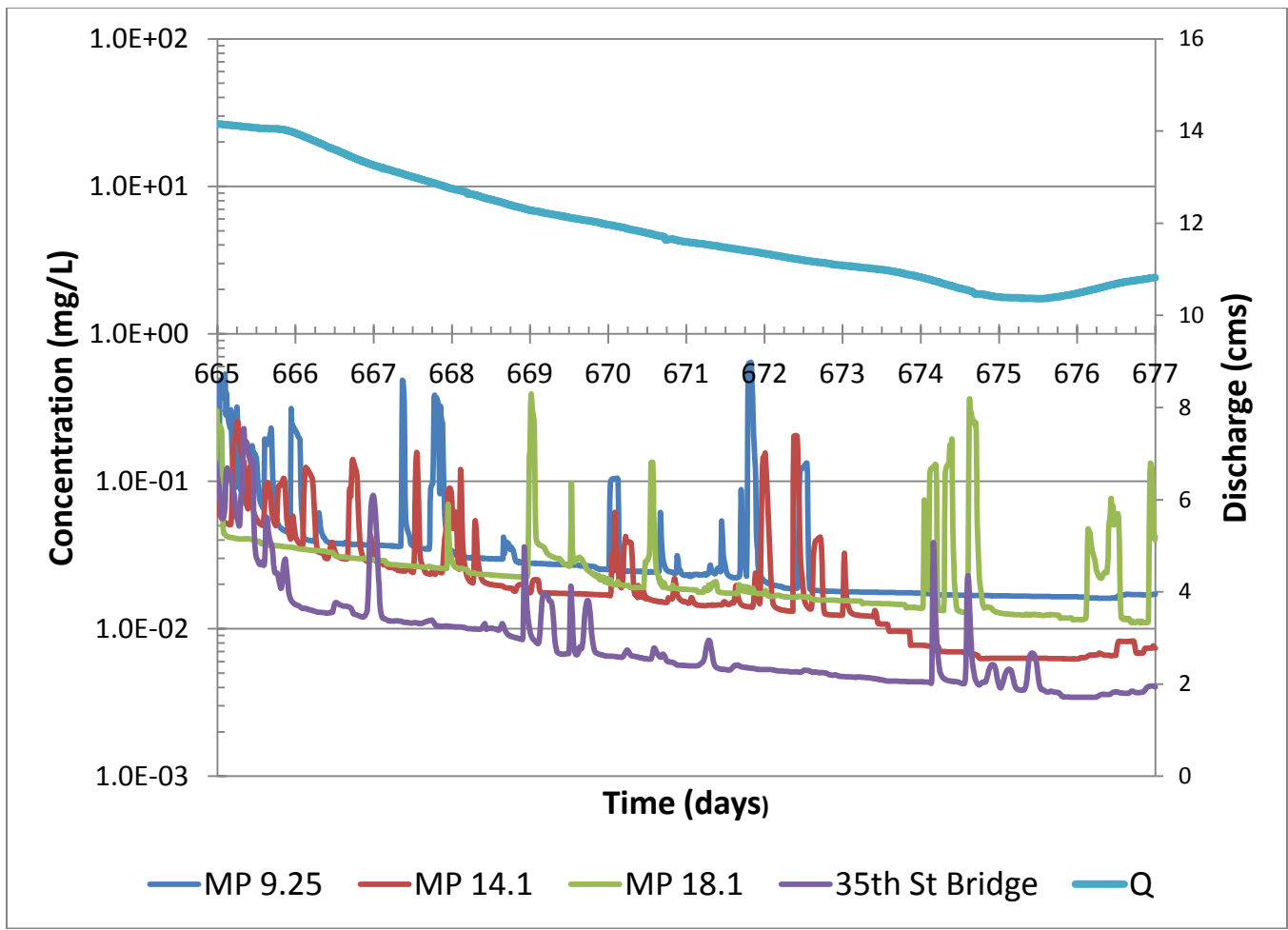


Figure 3-4 Total OPA Concentration Time Series at the Specified Four Locations. Day 665 corresponds to Oct 29.

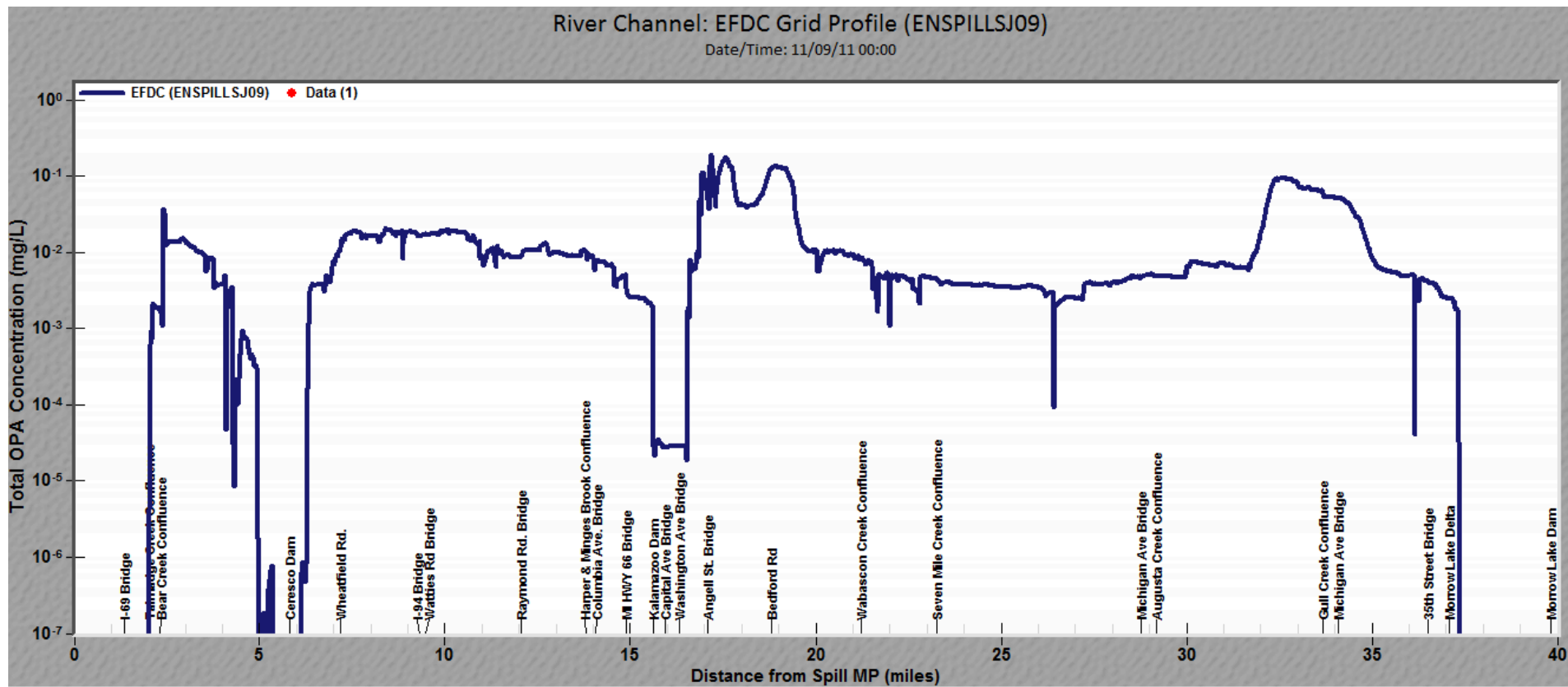


Figure 3-5 Longitudinal Total OPA concentrations at the end of the 13-day simulation

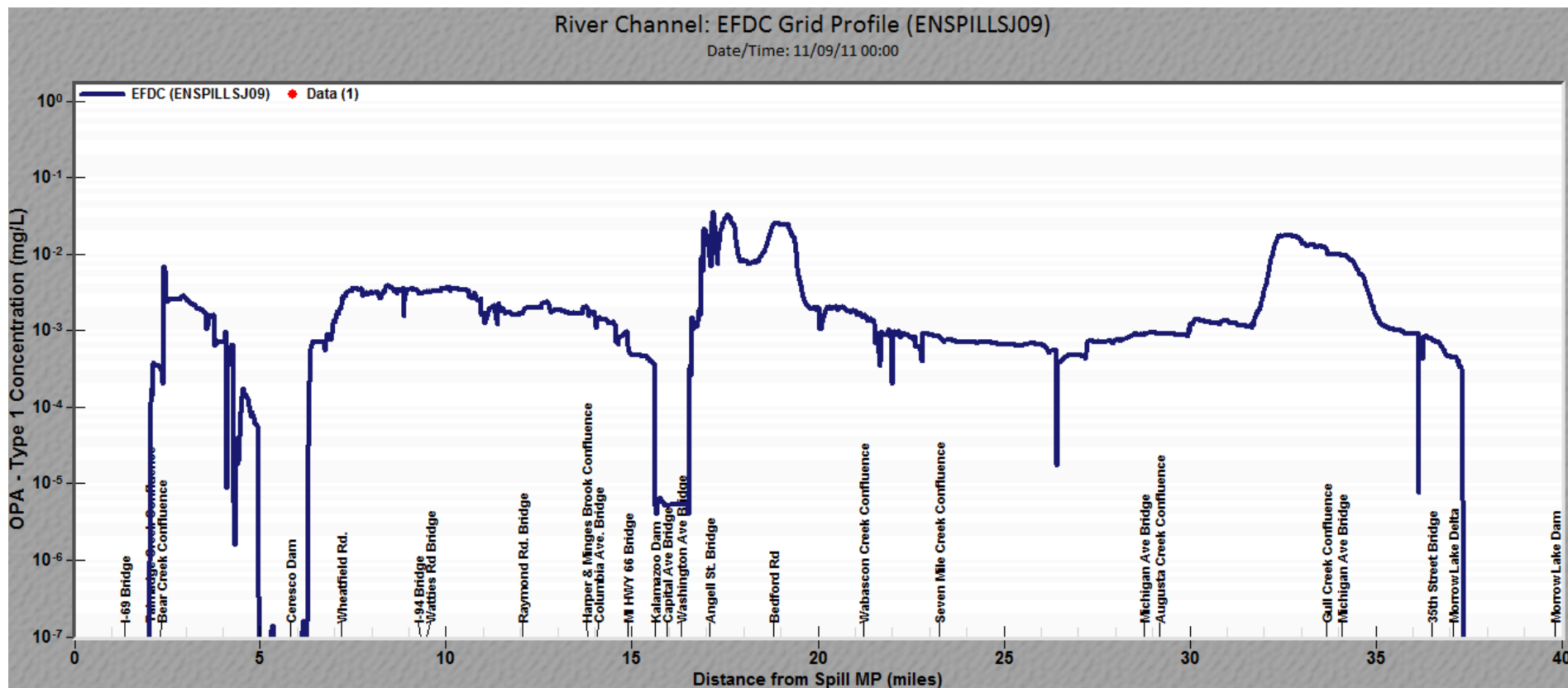


Figure 3-6a Longitudinal OPA concentrations for Type 1 OPA at the end of the 13-day simulation

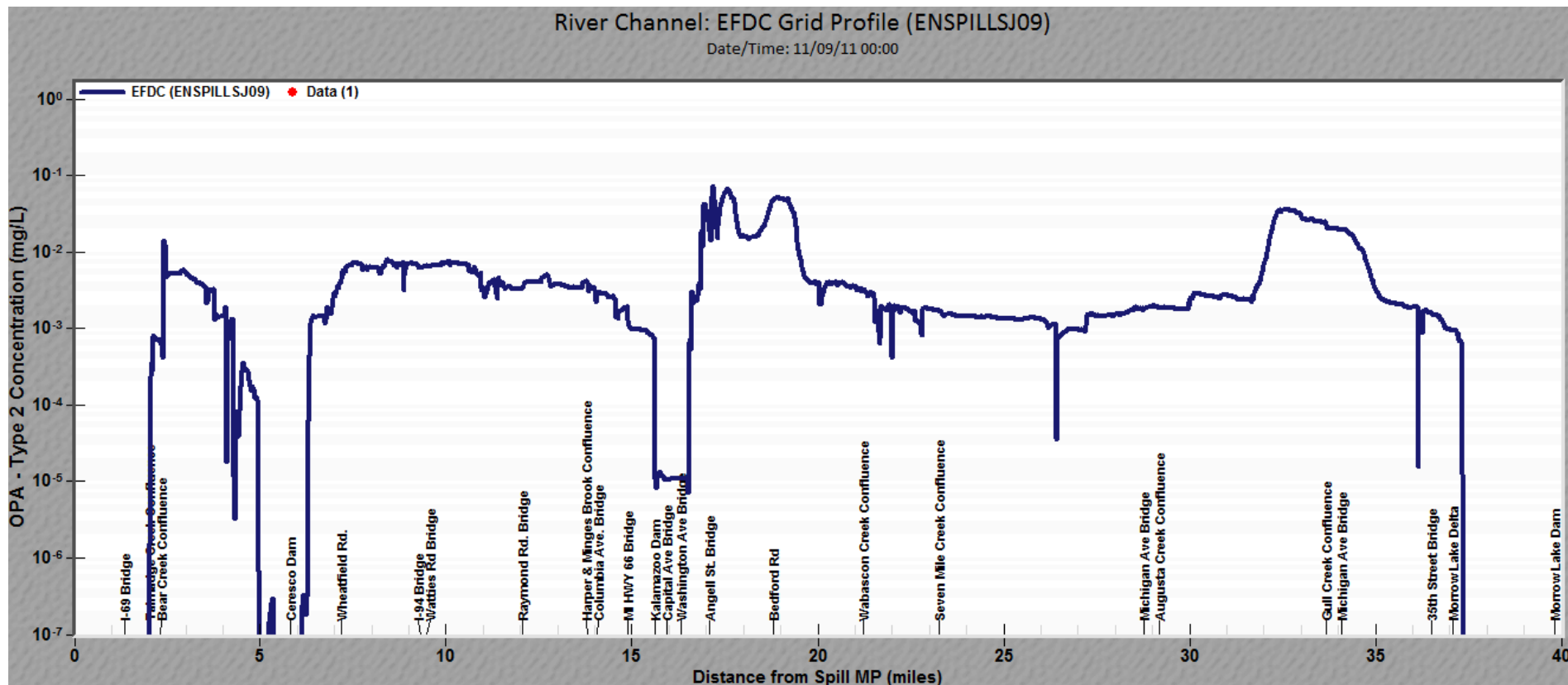


Figure 3-6b Longitudinal OPA concentrations for Type 2 OPA at the end of the 13-day simulation

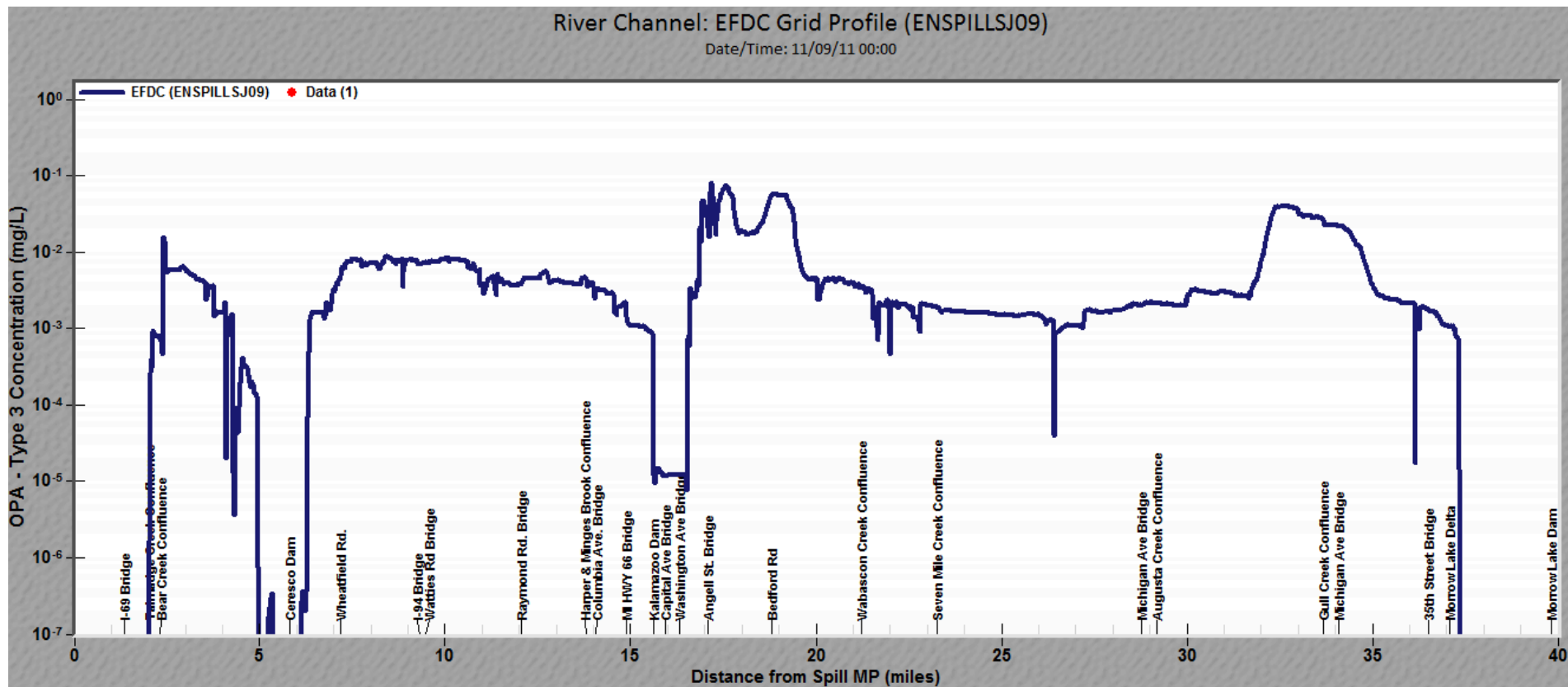


Figure 3-6c Longitudinal OPA concentrations for Type 3 OPA at the end of the 13-day simulation

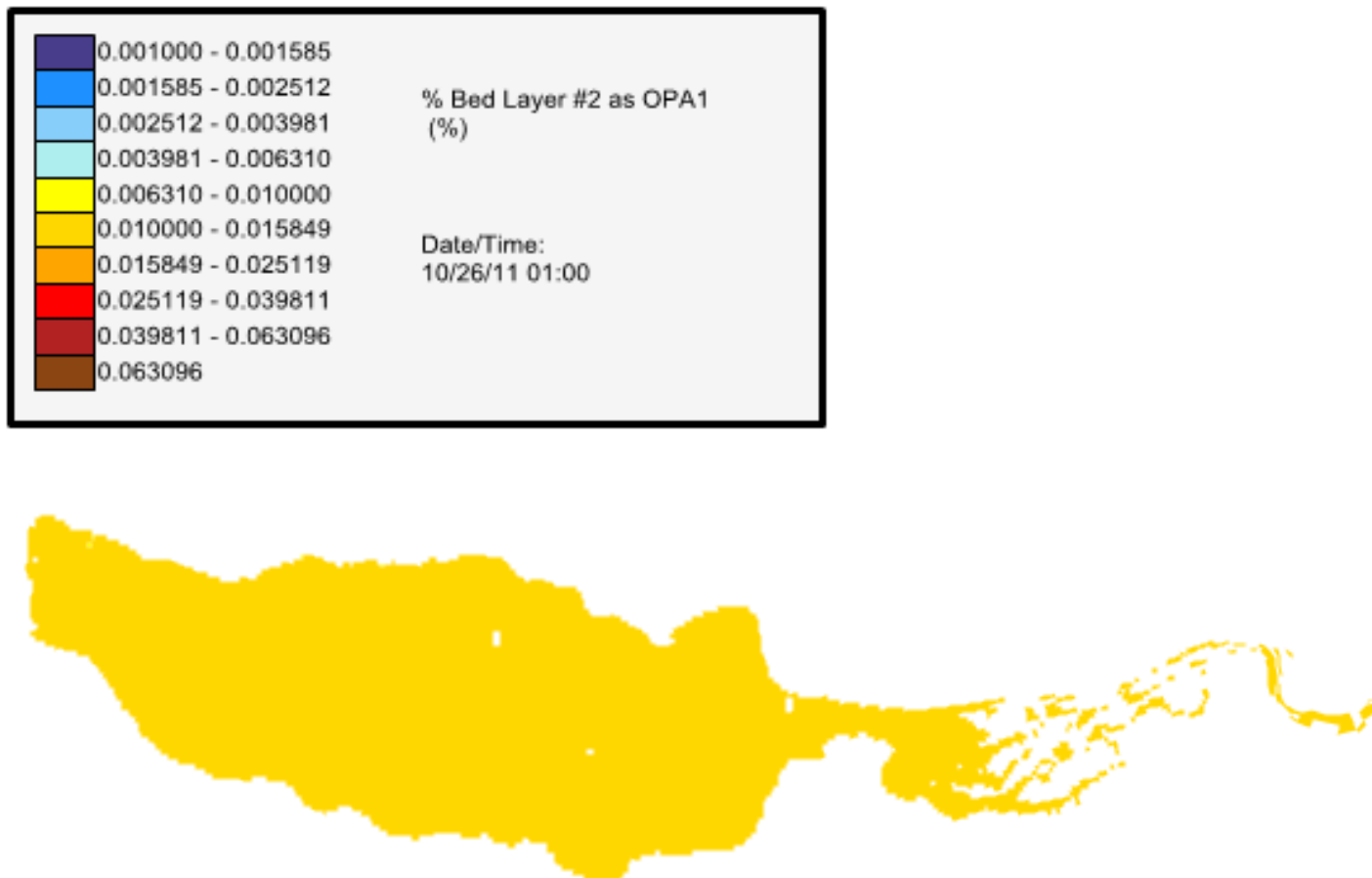


Figure 3-7a Percentages of OPA Type 1 in Bed Layer 2 at the beginning of the 13-day simulation

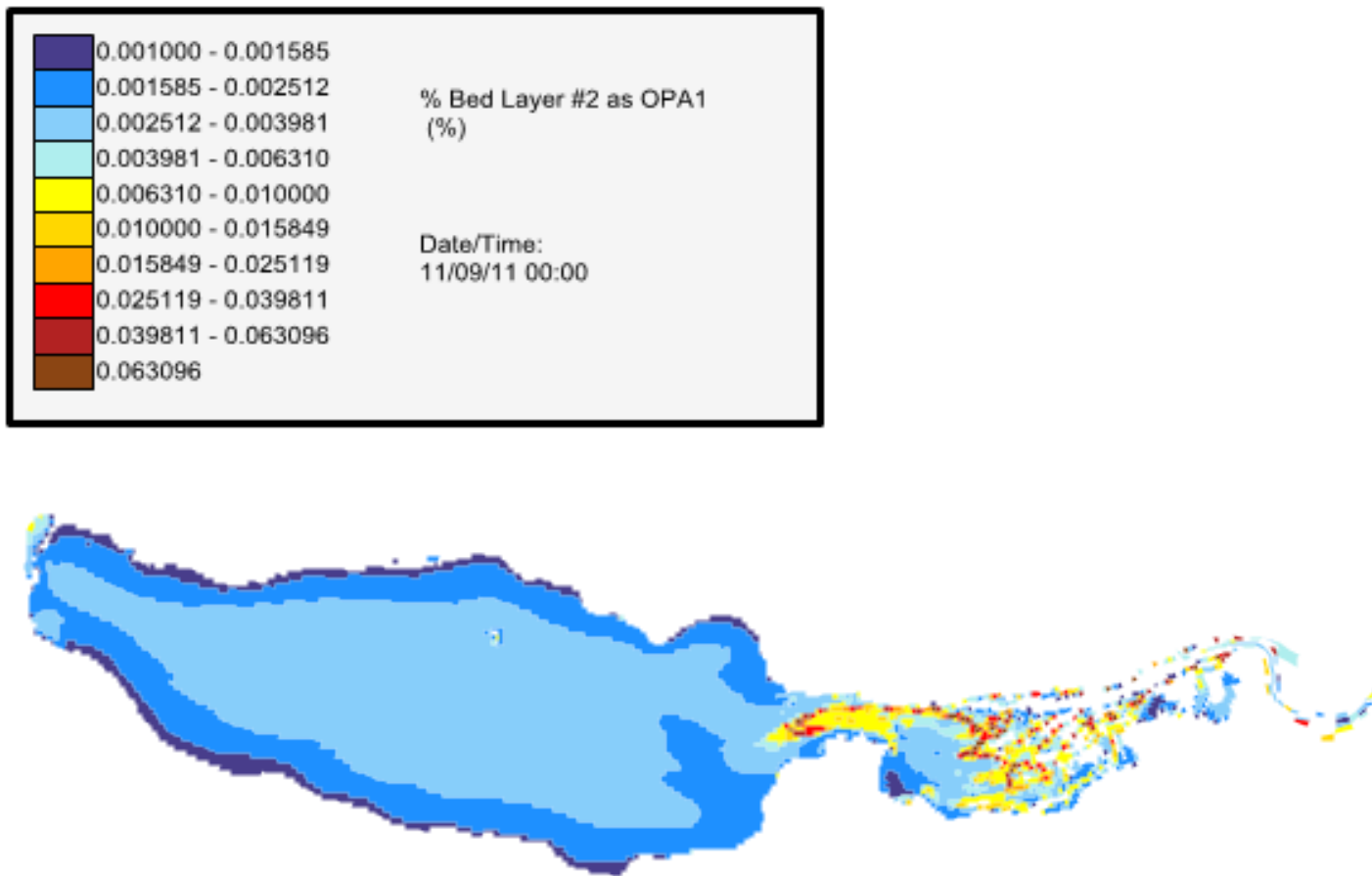


Figure 3-7b Percentages of OPA Type 1 in Bed Layer 2 at the end of the 13-day simulation



Figure 3-8a Percentages of OPA Type 2 in Bed Layer 2 at the beginning of the 13-day simulation



Figure 3-8b Percentages of OPA Type 2 in Bed Layer 2 at the end of the 13-day simulation



Figure 3-9a Percentages of OPA Type 3 in Bed Layer 2 at the beginning of the 13-day simulation

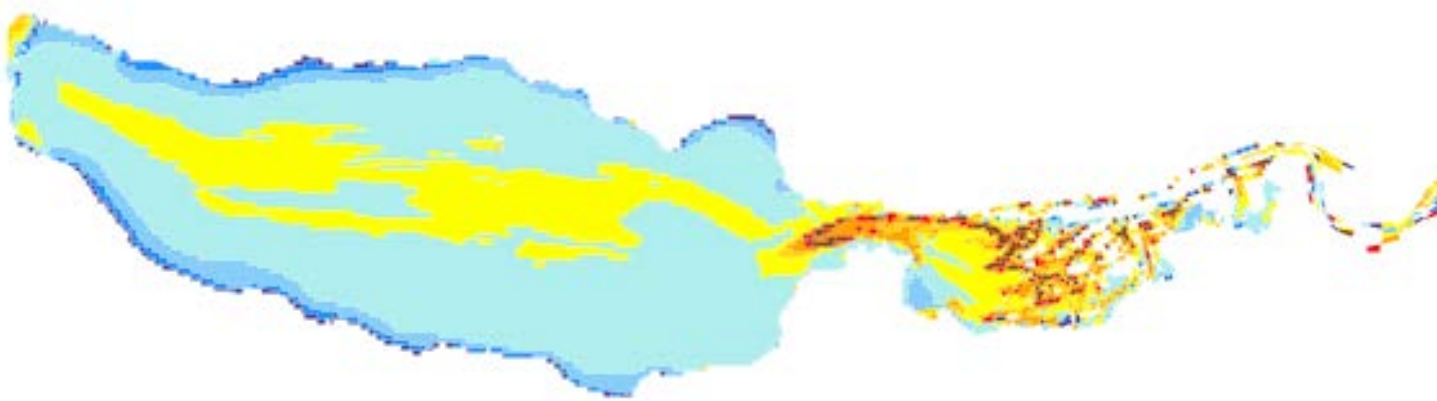


Figure 3-9b Percentages of OPA Type 3 in Bed Layer 2 at the end of the 13-day simulation



Figure 3-10 Change in Bed Elevation over the 13-day simulation

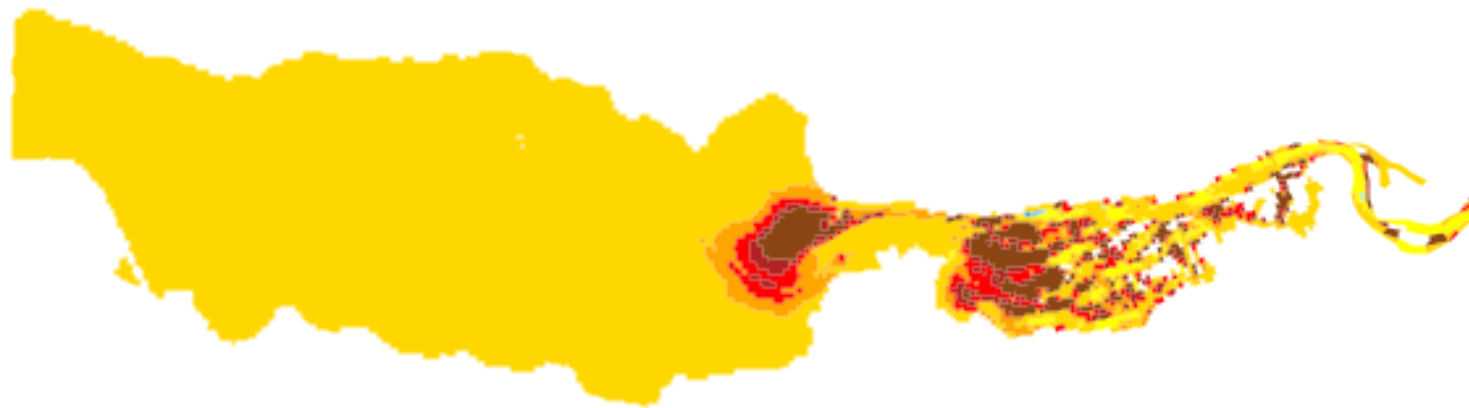
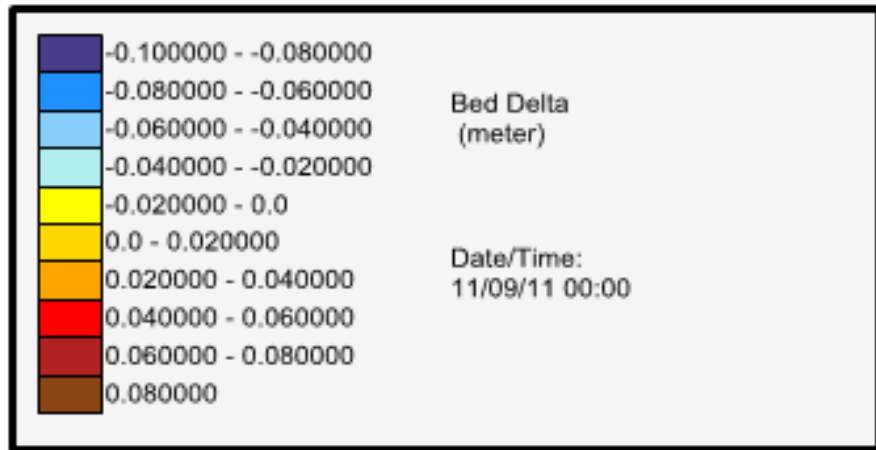


Figure 3-11 Change in Bed Elevation from -0.1 to 0.1 m over the 13-day simulation

3 in bed layer 2, respectively. As seen in these six figures, the percentages of all three types of OPA at the end of the model simulation are lower than at the beginning of the simulation. Figure 3-10 shows the total change in bed elevation over the 13-day model run, while Figure 3-11 shows the bed elevation change from -0.1 to 0.1 m. The latter figure allows the depositional pattern in Morrow Lake to be visualized. As seen and as expected, the reservoir is net depositional, with the bed change being between 0 and 0.02 m over the vast majority of the area. Figures 3-7b, 3-8b and 3-9b show that the percentages of all three OPA types in general decrease over the 13-day model run. This is caused by the deposition of new sediment in this impoundment. Deposition of suspended OPAs occurs as well, but the depositional rate is less than that for suspended sediment because the settling velocities of the three OPA types are less than for the sediment size classes and the concentration of suspended sediment is greater than that of the OPA classes. As a result, the mass of sediment that deposits is greater than the mass of OPAs that deposit, so the percentages of the OPA types in the bed decreases over the simulated 13-days. While there are no data to verify these model results, at least they are qualitatively reasonable.

4 Conclusions and Recommendation

The conclusions from this model development study are summarized below.

- Over the 13-day model run, 98 percent of the total mass of sediment and OPAs were conserved. Based on the extensive experience of the **authors' in the use of EFDC over the past 15 years, this is an excellent** result.
- The 13-day simulation of the transport of five sediment size classes and three OPA classes demonstrated the ability of the model to represent the transport of OPA as well as that of mixed sediment in a relatively large model domain, that being the 38-mile reach of the Kalamazoo River.
- The initial model results for the 13-day simulation period predict entrainment of all three OPA types for most non-impounded river locations, whereas deposition is predicted for the impounded areas.
- The simplified OPA transport module developed in this study is viewed as a first generation model, upon which more advanced modeling algorithms of OPA formation, transport, deposition, resuspension and potentially breakup can be built during future studies.
- It is recommended that a larger flow event, such as the April 2013 flood, be simulated to further test the new OPA transport module.
- A future study should also include the collection of a sufficient database to enable a prototype scale verification of the sediment and OPA transport models.

References

- Arega, F., and E.J. Hayter. 2008. “**Coupled** consolidation and contaminant transport model for simulating migration of contaminants through sediment and a **cap**.” *Journal of Applied Mathematical Modelling*, 32:2413–2428.
- Belore, R. 2010. “Properties and fate of hydrocarbons associated with the hypothetical spills at the marine terminal and in the confined channel assessment area,” Enbridge Northern Gateway Project, SL Ross Environmental Research LTD., Ottawa, Ontario.
- Cheng, N.S. 1997. “**Simplified settling velocity formula for sediment particles.**” *Journal of Hydraulic Engineering*, 123(2):149-152.
- Dollhopf, R.H., F.A. Fitzpatrick, J.W. Kimble, D.M. Capone, T.P. Graan, R.B. Zelt, and R. Johnson. 2014. “Response to heavy, non-floating oil spilled in a Great Lakes river environment: a multiple-lines-of-evidence approach for submerged oil assessment and recovery,” *Proceedings, 2014 International Oil Spill Conference*, Savannah, GA, May 7-9, 2014, 434-448.
- Fitzpatrick, F.A, R. Johnson, Z. Zhu, D. Waterman, R.D. McCulloch, E.J. Hayter, M. Garcia, M. Boufadel, T. Dekker, J.S. Hassan, D.T. Soong, C. Hoard, and K. Lee. 2015. “Integrated Modeling Approach for Fate and Transport of Submerged Oil and Oil-Particle Aggregates in a Freshwater Riverine Environment,” *Proceedings of the 10th Federal Interagency Sedimentation Conference*, Reno, NV.
- Hoard, C.J., K.K. Fowler, M.H. Kim, C.D. Menke, S.E. Morlock, M.C. Pepler, C.M. Rachol, and M.T. Whitehead. 2010. “Flood-Inundation Maps for a 15-Mile Reach of the Kalamazoo River from Marshall to Battle Creek, Michigan,” *U.S. Geological Survey Scientific Investigations Map 3135*: 6 p. pamphlet, 6 sheets, scale 1:100,000.
- James, S.C., C.A. Jones, M.D. Grace, and J.D. Roberts. 2010. “Advances in sediment transport modelling.” *Journal of Hydraulic Research*, 48: 6, 754-763.
- Jones, C.A., and W. Lick. 2001. “**SEDZLJ: A sediment transport model.**” *Final Report*. University of California, Santa Barbara, California.

King, T.L., B. Robinson, M.C. Boufadel, and K. Lee. 2014. "Flume tank studies to elucidate the fate and behavior of diluted bitumen spilled at sea," *Marine Pollution Bulletin*, 83(1), 32-37.

Lee, K. 2002. "Oil-particle interactions in aquatic environments: influence on the transport, fate, effect, and remediation of oil spills," *Spill Science and Technology Bulletin*, 8(1), 3-8.

Lee, K., M. Boudreau, J. Bugden, L. Burrige, S.E. Cobanli, S. Courtenay, S. Grenon, B. Hollebhone, P.Li Kepkay, M. Lyons, H. Niu, T.L. King, S. MacDonald, E.C. McIntyre, B. Robinson, S.A. Ryan, and G. Wohlgeschaffen. 2011. "State of Knowledge Review of Fate and Effect of Oil in the Arctic Marine Environment," Report for the National Energy Board of Canada, Arctic Roundtable: State-of-Knowledge Review of Fate and Effects of Oil in Arctic Offshore. Fisheries and Oceans Canada. 259 p.

Lee, K., J. Bugden, S. Cobanli, T. King, C. McIntyre, B. Robinson, S. Ryan, and G. Wohlgeschaffen. 2012. "UV-Epifluorescence microscopy analysis of sediments recovered from the Kalamazoo River," Dartmouth, Nova Scotia, Centre for Offshore Oil, Gas and Energy Research (COOGER) Report, October 24, 2012.

Limnotech. 2014. "Kalamazoo River Hydrodynamic and Sediment Transport Model Documentation," **Ann Arbor, MI.**

McNeil, J., C. Taylor, and W. Lick. 1996. "Measurements of the erosion of undisturbed bottom sediments with depth." *Journal of Hydraulic Engineering*, 122(6):316-324.

Perkey, D.W., S.J. Smith, and T. Kirklin. 2014. "Cohesive Sediment Erosion Field Study: Kalamazoo River," **Letter Report, U.S. Army Engineer Research and Development Center, Coastal and Hydraulics Laboratory, Vicksburg, MS.**

Sanford, L.P. 2008. "Modeling a dynamically varying mixed sediment bed with erosion, deposition, bioturbation, consolidation, and armoring." *Computers & Geosciences*, 34(10):1263-1283.

Van Niekert, A., K. Vogel, E. Slingland, and J. Bridge. 1992. "Routing of heterogeneous sediments over movable bed: Model development," *J. Hydraulic Engineering*. 118(2), 246-263.

Van Rijn, L.C. 1984. "Sediment Transport: part i: bedload transport; part ii: suspended load transport: part iii: bed forms and alluvial

roughness.” *Journal of Hydraulic Engineering*, 110(10): 1431-1456; 110(11): 1613-1641, 110(12): 1733-1754.

Waterman, D., and M.H. Garcia. 2014. “Laboratory Tests of Oil-Particle Interactions in a Freshwater Riverine Environment with Cold Lake Blend Weathered Bitumen,” Technical Report, Ven Te Chow Hydrosystems Laboratory, University of Illinois at Urbana-Champaign.

Waterman, D., D. Fytanidis, and M.H. Garcia. 2014. “Kalamazoo River In Situ Flume Bed Erosion Study, Report, Ven Te Chow Hydrosystems Laboratory, University of Illinois at Urbana-Champaign.

Zhao L., M.C. Boufadel, E. Adams, S.A. Socolofsky, and K. Lee. 2014. “Simulation of Scenarios of Oil Droplet Formation in the Deepwater **Horizon blowouts,**” *Marine Pollution Bulletin* (submitted).

Appendix A

Process of overlaying oiling categories onto SEDZLJ bed layers for EFDC modeling

Estimating OPA concentrations in riverbed sediment for SEDZLJ modeling simulations was based on data collected for EPA's study to quantify the remaining oil in the river as of spring/summer 2012.

The first step was to divide the riverbed in terms of its layering in the SEDZLJ model. The riverbed was grouped into five layers based on experience of the modelers:

- Layer A = 0-2 cm
- Layer B = 2-5 cm
- Layer C = 5-10 cm
- Layer D = 10-18 cm
- Layer E = 18-30 cm

An available GIS layer that delineated light/none and heavy/moderate groupings of oiling were used to represent the spatial distribution of Line 6B oil in riverbed sediment. This same layer was used for the EPA oil quantification study and represented oiling conditions in the river based on Spring 2012 poling assessment results. Using summer 2012 streambed core results for Line 6B oil concentrations, Ron Zelt (USGS-Nebraska Water Science Center, written commun., June 2014) calculated the average concentration of Line 6B in 0.1-ft increments in heavy/moderate and light/none areas similar to what was done for the oil quantification study. The individual 0.1-ft increments were averaged for the five SEDZLJ layers, resulting in two possible oil concentrations for each of the five layers. These are shown in Table A-1.

Table A-1 Oil Concentrations for the Five Sediment Bed Layers

Line 6B Median Oil Concentration (mg/kg) from quantification cores	Top Layer	Layer B	Layer C	Layer D	Layer E
Heavy/Moderate	349	217	211	217	172
Light/None	237.5	129.5	131	128	110

The GIS layer with the oiling categories was overlain with a GIS layer of the EFDC model grid by Weston, Inc. From the resulting overlay, if greater than 20 percent of a grid cell was categorized as heavy/moderate, that grid cell was labeled as heavy/moderate. If less than 20 percent of a grid cell was categorized as heavy/moderate, than that grid cell was labeled as light/none.

The concentration of OPA in each of the 10 possible layers was based on relative proportion of oil in each type of OPA. As shown in Table 2-1, in the final version of the modeling, three types of OPA were included. The concentration of oil was split evenly amongst the types. Table A-2 shows the percentages of oil and OPA that were used for the SEDZL layers.

Table A-2 Oil and OPA Percentages used for the Five Sediment Bed Layers

	Equal Split Mass (oil) (mg/kg)	Type 1 OPA (%)	Type 2 OPA (%)	Type 3 OPA (%)
Heavy/Moderate Top layer (0-2 cm)	116.333	0.01258	0.02544	0.02855
Heavy/Moderate Layer B (2-5 cm)	72.333	0.00782	0.01582	0.01775
Heavy/Moderate Layer C (5-10 cm)	70.333	0.00761	0.01538	0.01726
Heavy/Moderate Layer D (10-18 cm)	72.333	0.00782	0.01582	0.01775
Heavy/Moderate Layer E (18-30 cm)	57.333	0.00620	0.01254	0.01407
Light/None Top layer (0-2 cm)	79.167	0.00856	0.01731	0.01943
Light/None Layer B (2-5 cm)	43.167	0.00467	0.00944	0.01059
Light/None Layer C (5-10 cm)	43.667	0.00472	0.00955	0.01072
Light/None Layer D (10-18 cm)	42.667	0.00461	0.00933	0.01047
Light/None Layer E (18-30 cm)	36.667	0.00397	0.00802	0.0090

